DOR:

Research Paper

Experimental Investigation of the Effect of Using Tools with Tapered Pins in Friction Stir Welding (FSW) of AA6061-T6 Aluminum Alloy

Saleh Al-Khathour[1], Maziar Mahdipour Jalilian[1*], Mahdi Karami Khorramabadi[2]
[1]Department of Mechanical Engineering, Kermanshah Branch, Islamic Azad University, Kermanshah, Iran
[2]Department of Mechanical Engineering, Khorramabad Branch, Islamic Azad University, Khorramabad, Iran
[*]Email of Corresponding Authors: maziar.1986.2000@gmail.com
Received: February 13, 2024; Accepted: May 1, 2024

Abstract
The present study investigated the effect of using tools with tapered pins in Friction Stir Welding (FSW) of AA6061-T6 aluminum alloy. Two techniques named conventional FSW and Refill Friction Stir Welding (RFSW) were used for this purpose. Five tools with different tapered angles (0, 5, 10, 15, and 20 degrees) were used. To study the mechanical properties, tensile, three-point bending, and Vickers microhardness tests were performed. Macrographic and microstructural tests were also used to investigate the metallurgical properties of the welded samples. Based on the results, it was found that the key factors determining the ductility and strength of the welded specimens are the type of welding process (conventional FSW or RFSW) and the geometry of the tool pin (straight or tapered pin). Furthermore, it was found that all specimens welded by RFSW have higher tensile strength and elongation than the samples welded by conventional FSW.

Keywords
Friction Stir Welding (FSW), Tool Geometry, Tapered Pin, Aluminum Alloy, Strength of Weld

1. Introduction

Today, safety is of great importance in industrial designs. In this way, many factors and parameters must be considered by the designer. Engineers are always trying to take these factors into account, and extensive measures and research have been done to improve these conditions. Among these cases, one can mention the type and quality of joining used in industries. The choice of the joining technique of the parts depends entirely on the function of the part. Normally, according to the type of expectation from the desired product, the connection technique is selected and performed, which is influenced by factors [1]. Friction Stir Welding (FSW) is a solid-state joining process. Different techniques are used to perform the FSW process, one can mention Reverse Dual-rotation Friction Stir Welding (RDR-FSW), performing the FSW process using tandem tools, Multi-Pass FSW (MP-FSW) with reverse tool rotation, and Parallel FSW. Li and Liu [2-4] investigated the RDR-FSW of the AA2019-T6 aluminum alloy process. Based on their findings, it was found that the use of this technique significantly increases the mechanical and metallurgical quality of the connection and reduces the force and torsional torque required to perform the process. Shi et al. [5] studied the thermomechanical modeling of the RDR-FSW process. Based on the results, it was found that the use of the RDR-FSW technique creates relative symmetry in the pattern of heat distribution and plastic flow in the

workpiece. The use of tandem tools was first proposed by Thomas et al. [6] at the Cambridge Welding Institute. In this method, two tools move in a line with a reverse rotational direction and form the welding process. According to the research results, this method has significant advantages over the usual FSW process, such as reducing the clamping force torque and defects and increasing the joint efficiency. Liu and Zhang [7] used the line re-welding technique to eliminate the groove defect. In the second step, they reversed the welding of the tool to rotate the tool. Based on the results, it was found that the use of this method eliminates defects and significantly increases joint efficiency. Kumari et al. [8] investigated the two-pass FSW by reversing the direction of tool rotation in the first and second passes. According to the reported results, the use of the MP-FSW technique with reverse rotation caused a significant increase in the mechanical properties of the joint. Jain et al. [9] investigated and numerically simulated the FSW with inverted inline twin-pin tools and inverted direction. It was found that the use of this tool increases the peak temperature of the process and symmetry of the strain distribution and strain rate in the process and reduces the defects of the FSW process.

The present study investigated the effect of using tools with tapered pins in Friction Stir Welding (FSW) of AA6061-T6 aluminum alloy. Two techniques named common FSW and RP- FSW backward were used for this purpose. Five tools with different tapered angles (0, 5, 10, 15 and 20 degrees) were used. To study the mechanical properties, tensile, three-point bending, and Vickers microhardness tests were performed. Macrographic and microstructural tests were also used to investigate the metallurgical properties of welded samples. Based on the results, it was found that the determinant factors of ductility and strength of welded specimens are the type of welding process (FSW or RP- FSW) and the geometry of the tool pin (simple or tapered pin). Also, it was found that all specimens welded by RP- FSW have higher tensile strength and elongation than the sample welded by conventional FSW.

2. Materials and Methods

2.1 Materials

Hot work tool steels have been designed for applications where the temperature is above 316 ° C. Cold work tool steels usually soften and their strength decreases when exposed to high temperatures. Also, high-speed steels do not soften at such temperatures, but their toughness and resistance to heat shock are not suitable for use at high temperatures. Hot work tool steels have relatively low carbon with maximum toughness and elements such as Mo, W, and Co are used to resist softening at high temperatures. Adding vanadium to steel improves its thermal resistance. Vanadium is added to increase wear resistance. Hot work tool steels are divided into two groups. The main element of the first group is molybdenum and the main element of the second group is tungsten. Molybdenum steels usually show better toughness and thermal resistance than the tungsten group. This category is mostly used for hot work tool steels. Hot work tool steels are typically used to make hot forming tools for ferrous and non-ferrous alloys at temperatures above 200 ° C. Because, in the FSW process, very large thermal cycles are created during the process, a tool must be used to maintain its function at high temperatures and its mechanical properties do not change. In the present study, H13 hot work tool steel was used to make all the tools. This hot-rolled steel is used in most research by researchers

as a raw material for making tools of the FSW process. Table 1 shows the chemical composition of H13 hot work tool steel.

Table 1. Chemical composition of hot work tool steel H13 (wt %)

Cr	Mo	Si	V	C	Ni	Cu	Mn	P	S
4.75-5.5	1.1-1.75	0.8-1.2	0.8-1.2	0.32-0.45	0.3	0.25	0.2-0.5	0.03	0.03

To make the tools of the present study, two shafts made of H13 hot work tool steel with a diameter of 20 mm and a length of 25 cm were prepared shown in Figure 1.

Figure 1. H13 shafts for tool making

After preparing the raw material, and designing and preparing the dimensional drawings of the desired tools, a Cincinnati CNC milling machine made in the United States was used for the production of the tools. It should be noted that to increase the dimensional accuracy of the tools in the present study, it was not possible to use a conventional milling machine to make the tools. By changing the geometric parameters of the tool, the material flow created in the process changes significantly, and this change in the pattern and volume of the flow changes the quality of the joint. One of the important parameters of tool geometry is the tapered angle of pins. Based on research, it has been determined that the use of tapered cylindrical tools compared to simple cylindrical tools will increase the quality and mechanical properties of the joint. By creating an optimal tapered angle at the tool pin, the temperature gradient in the connecting components changes, and due to this gradient change, the plastic flow volume and the horizontal and vertical flow patterns of the material also change, which leads to improving the quality of the joint. Also, the defects of the process are eliminated to a high degree. By changing the tapered angle of the pin, the volume of flow at the workpiece floor changes which increases the possibility of a proper and defectless joint in this area. Another possible way to reduce process defects and increase the quality of welding in the floor area of the workpiece is to change the geometry and joint-making procedure. In the present study, tapered tools have been used to perform P-FSW. Figure 2 shows a schematic of a tool with a tapered angle and a simple tool. To design tools, 5 angles of 0, 5, 10, 15, and 20 degrees were used. These tools are shown in Figure 2.

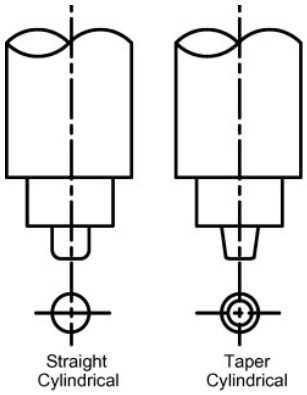

Figure 2. Schematic of simple tools and tapered tools

The tool undergoes relatively large mechanical and thermal stresses in the welding process. These stresses increase corrosion and defects in the tool. Thermal hardening is typically used to extend the life of the tools. In the present study, all tools were subjected to a cycle of thermal hardening. To do this, the following steps were performed.

Preheating stage: The preheating stage of the tools took place in two different stages. In the first stage, the temperature of the tool increased with a temperature rate of 222 ° C / h to reach the temperature of 650 ° C. It should be noted that after reaching this temperature, the tool was kept at this temperature for one hour. In the second phase of the preheating, the temperature of the tools was increased from 650 ° C to 850 ° C with a temperature rate of 222 ° C / h and kept at this temperature for one hour.

Customization stage: In this stage, the temperature increased immediately from 850 degrees to 982 degrees centigrade, and the tools were kept at this temperature for 90 minutes.

Quenching stage: In this stage, a large tank of oil was prepared and the tools were taken out of the furnace and released into the tank. After cooling the tools to 450 degrees centigrade, the tools were taken out of the tank and the cooling process was continued in the open air until they reached room temperature.

Aluminum AA6061 is one of the hard alloy aluminum alloys, of which magnesium and silicon are the main alloying elements. This alloy was developed in 1935. Important features of this alloy include its welding and extrusion capability; Its extrusion-ability has led to its widespread use in the extrusion of various sections. In the present study, AA6061-T6 aluminum alloy has been used to perform the P-FSW process. These alloys were provided from Tehran Aluminum Market. Table 2 and Table 3 show the chemical composition and mechanical properties of this alloy.

Table 2. Chemical composition of AA6061-T6 alloy (%)

Al	Mg	Si	Cu	Fe	Cr	Mn	Zn	Ti
Balance	0.81	0.61	0.29	0.2	0.13	0.03	0.02	0.01

Table 3. Mechanical properties of AA6061-T6 alloy

Yield Stress (MPa)	UTS (MPa)	Elongation (%)
268	330	17

Purchased sheets were prepared in a thickness of 5 mm. For all workpieces of P-FSW, parts with dimensions of 5 mm × 50 mm × 120 mm have been used. To cut the parts, an industrial guillotine is used to smooth the edges of the parts so that there is no gap between the two edges of the workpiece during the buttwelding process.

2.2 Methods

After cutting and preparing the parts, a milling machine was used to perform the process of P-FSW. The most important features of this apparatus are a powerful 11 kW motor, tool rotation speed up to 2000 rpm, the ability to move the machine table in three directions, complete control using mechanical and adjustable equipment, the ability to assign a constant speed in three directions and the ability to set the angle of the spindle of the apparatus. The column of the machine is made of cast iron in the form of a box and inside it, the electric motor of moving mechanisms, gearbox, load mechanism, and the neck of the machine are mounted. The axle of the machine is the steel in which the milling blades are fixed. The gearbox is designed to change the rotational speed of the neck (axis). The load gearbox is used to move the table in three directions. To perform the process, in the first stage, the bottom plate (anvil) and the appropriate fixture were prepared. In the present study, two processes of FSW and P- FSW have been used to join the parts. The process of P- FSW has two different modes. These different modes are determined by the direction of rotation of the tool during the first and second passes of the weld. If the direction of rotation of the tool in the first and second passes of welding is such that the outer edges of the two pieces are at the RS and the weld nugget is at the AS, the AP-FSW is formed. In reverse, that is, when the outer edges of the workpiece are at the AS and the weld nugget is at RS, RP-FSW is formed. The schematic of the two processes RP-FSW and AP-FSW is shown in Figure 3.

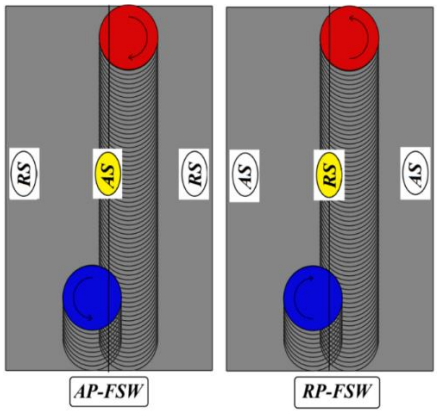

Figure 3. Schematic of RP-FSW and AP-FSW processes [10]

According to the research conducted by Ghiasvand et al. [10], the strength of the joints created by the RP-FSW is higher than the samples welded by the AP-FSW. Therefore, in the present study, among the P-FSW methods, only the RP-FSW method has been used. It should be noted that for welding in the first and second passes, an offset of 1 mm has been used. Because the process parameters (translation speed and rotational speed of the tool) play an important role in the mechanical quality and microstructure of the welded parts, these parameters must be set in their optimal values. For this purpose, following the proposed values in the literature survey [11], a translation speed of 60 mm/min

and a rotational speed of 1180 rpm have been used. Also, the tilt angle of the tool was equal to 2 degrees and the penetration depth was equal to 0.1 mm. It should be noted that the same process parameters were used for all samples.

3. Experimental Tests

3.1 Tensile Test

To perform the tensile test, according to the standards, the SANTAM STM-250 (made in Iran) tensile testing apparatus of Malayer University was used. Because the surface conditions of the weld have not reached equilibrium because of thermal cycles at the 2 cm of the beginning and end of the welded area, tensile test specimens should be prepared after separating these parts from the rest of the weld specimen. The dimensions of the samples were prepared according to ASTM-E8M standard. Figure 4 shows the dimensions of the tensile test specimen. It should be noted that two tensile test specimens were prepared from each welded specimen and the output results are based on the average results of the two specimens. All tensile tests were performed in the form of controlled- displacement at a speed of 2 mm/min.

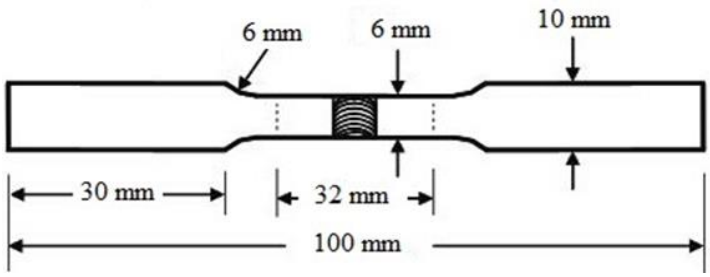

Figure 4. Dimensions of tensile test specimens

3.2 Three-point Bending Test

In the present study, a three-point bending test has been used to investigate the flexural behavior of welded specimens. This test is continued until a 90-degree angle is applied to the welding specimens. To perform this test, first, a three-point bending fixture was designed, and then bending tests were performed by a SANTAM STM-250 (made in Iran) machine located at Malayer University. The schematic of the dimensions of the three-point bending test specimens following ASTME190-92 is shown in Figure 5. The flexural strength of the specimen under flexural testing is obtained by the following equation. In this equation, the width of the beam, the length of the area between the two rollers, the maximum applied force, and the thickness of the beam are b, L, F, and d, respectively [13].

$$\sigma_f = \frac{3FL}{2bd^2} \quad (1)$$

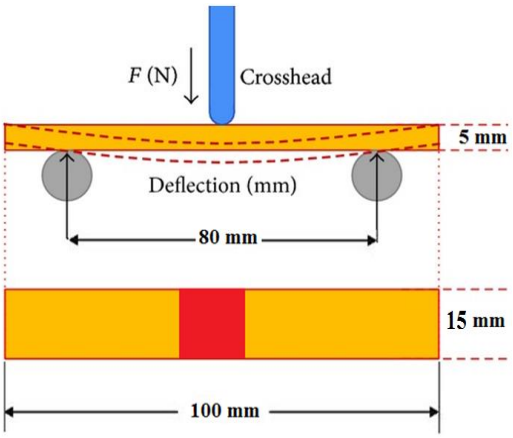

Figure 5. Dimensional schematic of three-point bending test specimens

3.3 Microhardness Test

In the present study, the Vickers microhardness test was used to calculate the cross-section hardness of welded specimens. To perform the hardness test, a cross-section was prepared for each welded specimen. Figure 6 shows the cutting positions of the specimen of the tensile, flexural, microhardness, and microstructure tests.

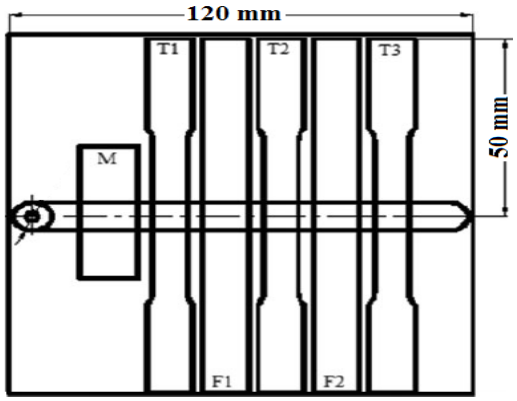

Figure 6. Cutting position of tension, bending, and microstructure specimens

Using sandpaper with grades of 220, 320, 500, 800, and 1200, the surfaces of the samples were polished and prepared for microhardness test, respectively. The microhardness test of the samples was performed by a microhardness apparatus made by American company Buehler in 30 seconds under a load of 50 grams and at room temperature. To record the micro-hardness distribution, 16 points at a depth of 1.5 mm and a direction perpendicular to the welding line were used for each sample. Figure 7 shows a schematic of the position of the microhardness recording points. Figure 8 also shows one of the samples prepared for microhardness testing.

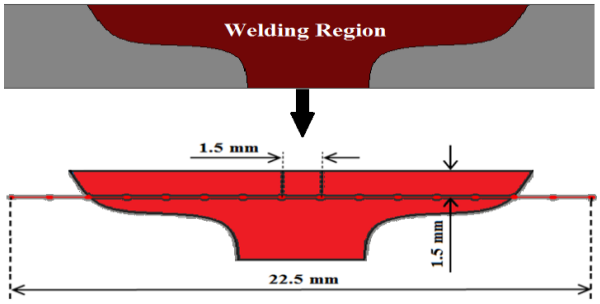

Figure 7. Schematic of the position of the points used to record the microhardness test

Figure 8: Schematic of a sample prepared for microhardness and microstructure tests

3.3 Metallography Test

In the present study, the samples were subjected to metallographic tests. Therefore, after welding, the pieces were cut in a direction perpendicular to the weld line for metallographic operations. The mounted samples were sanded with sandpapers at 400 to 2000 degrees. Then, the samples were first polished by a rotating machine using alumina powder and felt, and finally, the samples were polished with a solution of diamond liquid and felt for final polishing. The etching solution used for AA6061-T6 alloy was prepared by adding 1% by volume of hydrofluoric acid, 1.5% by volume of hydrochloric acid, 2.5% by volume of nitric acid, and 95% by volume of distilled water. The samples were etched in the prepared solution for 30 seconds. A Zeiss optical microscope was used to study the macrostructure and an electron microscope was used to study the microstructure of the welding section.

4. Results and discussion

In the presentation of research works, appropriate naming should be done for the samples to avoid confusion when presenting the results. For this purpose, six welding samples studied in this study have been named. Table 4 presents the studied models and the name of each model.

Table 4: The samples studied in this research

Sample's Name	Welding Process	Used Tool	Tapered angle
CF	Conventional FSW	Straight Cylindrical	0
RP-D0	RP-FSW	Straight Cylindrical	0
RP-D5	RP-FSW	Tapered Cylindrical	5
RP-D10	RP-FSW	Tapered Cylindrical	10
RP-D15	RP-FSW	Tapered Cylindrical	15
RP-D20	RP-FSW	Tapered Cylindrical	20

As mentioned, six different samples were deliberated for FSW of AA6061-T6 aluminum alloy parts. These examples vary in the type of process and the tool used. The first step in the welding process is the surface macro studying known as the visual inspection. The surface morphology of welded specimens with different welding tools and techniques (FSW and P-FSW) is investigated to identify possible defects in the surface of these specimens. As can be seen, the surfaces of all welded specimens are smooth with two different techniques and no lack of fill defect has been created on the surface of any of the specimens. There are also no visible cavities on the surface of any of the samples. In the RP-D10 and RP-D15 welded specimens, the welded surfaces are smooth and perfectly integrated, and no visible protrusions or cavities have been created in these specimens. However, it can be seen that in the other four welded specimens, protrusions and flash defects have been created in the marginal area of the weld line. In general, the flash defect is caused by increased heat and the presence of unstable plastic flow in the area of the welding edges. These protrusions are shown in Figure 9.

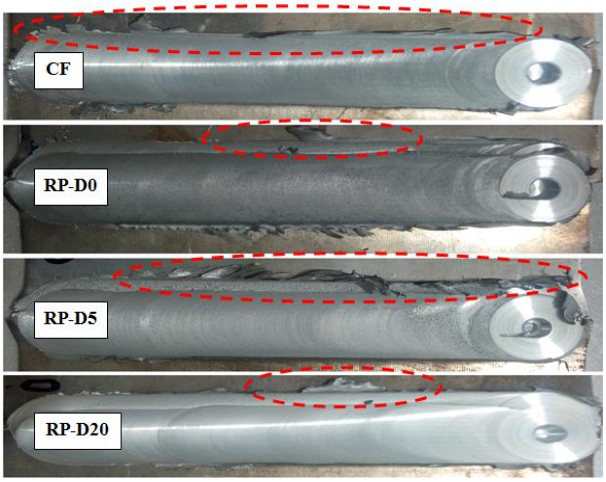

Figure 9. A flash defect on surfaces in some welding specimens

According to studies, the temperature distribution at AS is larger than RS and the maximum process temperature normally occurs in this region. For this reason, it was observed that in the welded specimens by the RP-FSW method, in which the AS is located in the marginal areas of the welding line, the flash defect was formed. This defect occurs outside the central area of the weld (RS), which is entirely related to AS. In specimens welded by the RP-FSW technique, the concentration of heat

and plastic flow is more stable in the central weld region (RS) and no significant surface defects occur in this region.

4.1 Tensile test results

The output of the tensile test specimens is a force-displacement diagram, which is converted to a stress-strain curve. Figure 10 shows some samples of tensile tests after the test. Also, Figure 11 shows the stress-strain curve of six welded specimens and the base metal. It should be noted that each of the stress-strain curves reported from the welding specimens is the result of an average of two tensile test specimens performed for each specimen.

Figure 10. Several samples were deliberated after the tensile test

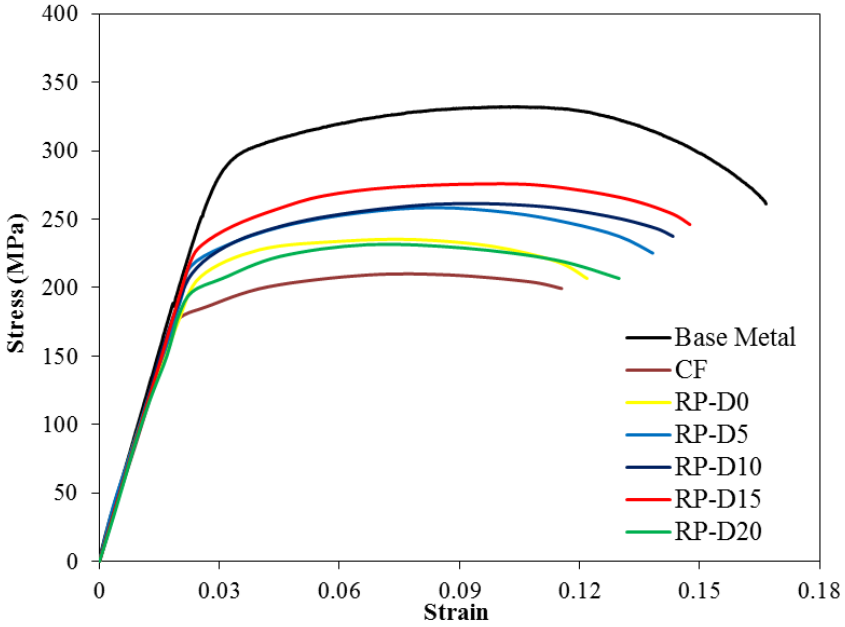

Figure 11. Stress-strain curves from tensile tests of welded specimens

According to Figure 11 and the results of the tensile test, it was found that the geometric shape of the tool pins strongly affects the mechanical quality of P-FSW joints and by changing the tapered angle of the pin, the tensile properties of the welded specimens change drastically. Based on the results of

tensile tests of specimens welded with different tools, it was found that the factor determining the ductility and strength of welded specimens is the type of welding process (FSW or P- FSW) and pin geometry (simple or tapered pin). The values of strength and ductility have a significant relationship with the two mentioned parameters. Based on the stress-strain curve presented in Figure 11, it was found that all specimens welded by the RP-FSW method have more strength and elongation than the specimen welded by the conventional FSW method.

4.2 Three-point bending tests results

The output of this test is a three-point graph of the bending force of the beam. Figure 12 shows the bending force diagrams of six welded specimens and the base metal diagram. Similar to the tensile test results, it should be noted that each of the bending force diagrams reported from the welding specimens is the result of an average of two three-point bending test specimens. It should be noted that all specimens were bent up to 27 mm. Some specimens failed to this point, and some did not fail and behaved in a ductile way.

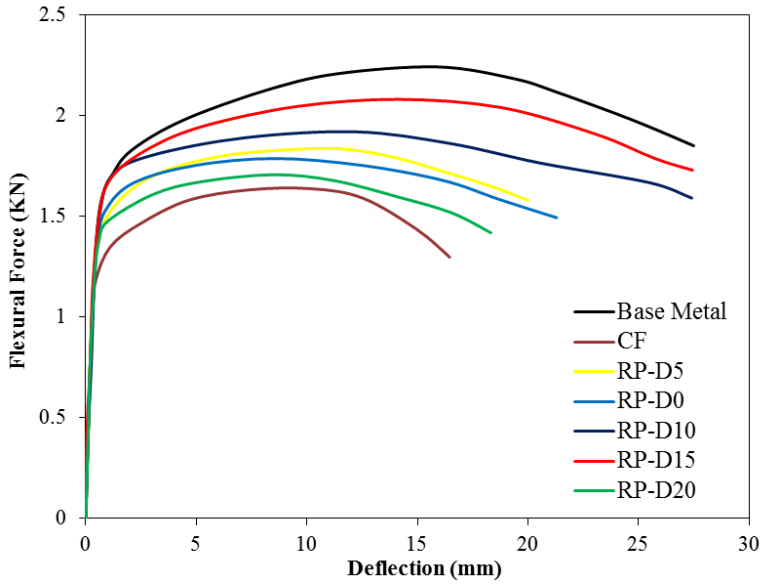

Figure 12. Flexural strength- deflection diagrams obtained from three-point bending tests of welded specimens

According to the results presented in Figure 12, it was found that the choice of welding process type and type of tool used for welding significantly affects the behavior of welding specimens under bending test. Based on the results of three-point bending tests, it was found that all samples welded by the P-FSW method show better bending behavior and have higher flexural strength compared to the sample welded by the conventional FSW method. Based on the obtained results, out of six welded samples, 2 samples of RP-D15 and RP-D10 of the bending test bed did not fail to bend up to 27 mm and showed the same behavior as the bending sample of the base metal.

4.3 Microhardness test results

For better comparison, the micro-hardness patterns of the samples are presented. Figure 13 shows the micro-hardness distribution of welded specimens by FSW and P-FSW methods using simple and tapered tools at different angles.

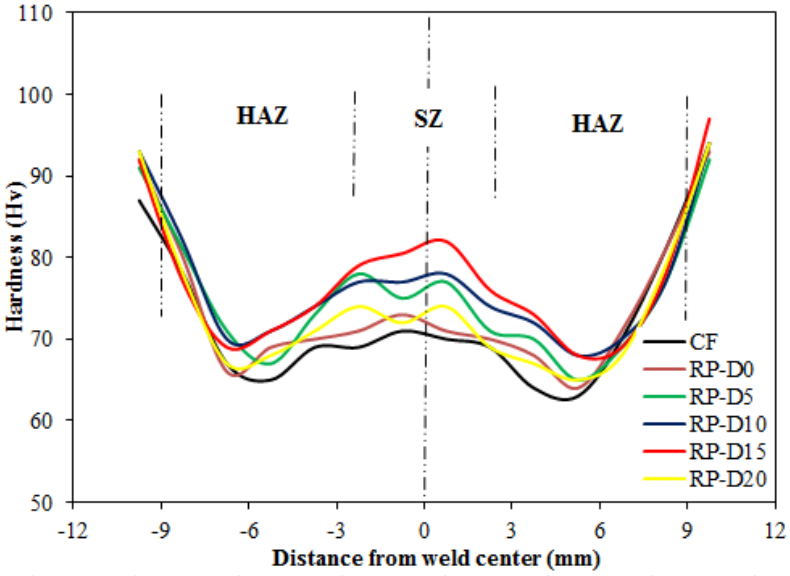

Figure 13. Cross-section microhardness distribution of welded specimens

According to the results presented in Figure 13, it was found that similar to FSW, in the conditions of using the P-FSW, the hardness pattern in all welding specimens is almost W-shaped. In all samples, the hardness of (SZ), the Thermo-Mechanical Affected Zone (TMAZ), and the Heat Affected Zone (HAZ) are significantly lower than the hardness of the base metal. In all samples, the hardness of SZ is higher than the adjacent areas due to the complete dynamic recrystallization that occurs in SZ and leads to the appropriate microstructure modification [12]. Regardless of the type of tool used for welding, the lowest hardness values occurred in the HAZ of samples. The range of hardness values of this zone in different samples is about 60-70. According to the microhardness patterns observed in the welded specimens by RP-FSW, the stiffness of SZ is directly related to the tapered angle of the used tool. As can be seen, tools with tapered angles of 15, 10, and 5 have the highest values of hardness in the central welding area, respectively, which is due to the significant increase in vertical plastic flow in this area resulting from the tapered feature of the tool. In addition to the horizontal flow, adding a tapered angle to the tool causes, a significant vertical flow to be formed in the center of the weld (weld nugget). This plastic flow increases the microstructural modifications and better distribution of grain size in these areas, and ultimately this finesse leads to an increase in the hardness of the weld nugget. It is observed that in other welding areas, almost the same hardness is observed due to the similar plastic flow density that different tools produce at distances farther from the weld nugget. It should be noted that the pattern observed in the hardness values of different specimens in SZ is in agreement with the results obtained in the field of two parameters of UTS and flexural strength.

4.4 Microstructure of welding specimen results

The study of the microstructure pattern of the weld zone and its granulation is known as a factor for the validation of mechanical test results. Therefore, in the present study, the microstructure images of the weld nugget of the studied samples have been presented. Figure 14 shows the different welding cross-sections of two samples, CF and RP-D15.

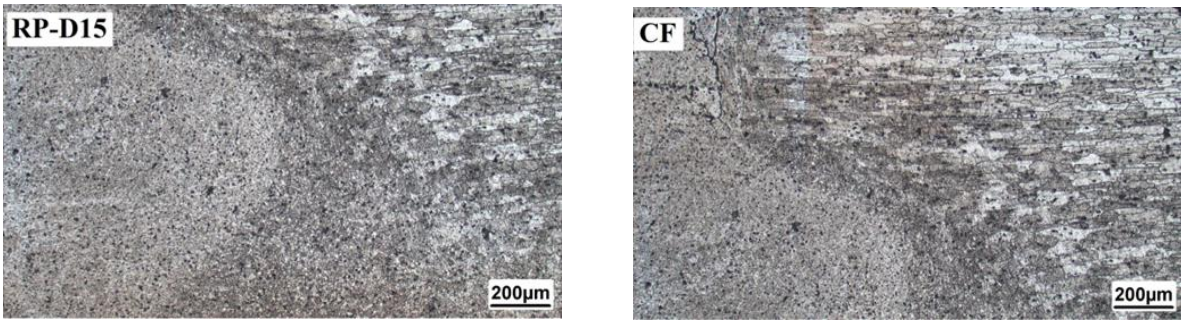

Figure 14. Different welding areas in two welded specimens CF and RP-D15 Figure

As can be seen, the separation of the SZ, TMAZ, and HAZ is well illustrated in the microstructural images of the weld cross sections of both specimens. In the HAZ, the studied samples did not recrystallize and the granulation of this zone is almost similar to the granules of the base metal, and only the granules are elongated to some extent. This elongation and deformation are following the results of other studies [12]. The TMAZ is formed by uniform temperature and deformation during the welding process. Deformed and somewhat recrystallized grains can be seen in this area. Recrystallization is rare in TMAZ due to insufficient temperature and less deformation intensity than in the central region. The SZ has the highest deformation among other regions and contains fine and coaxial grains resulting from complete dynamic recrystallization. This area experiences the highest temperature and plastic deformation during the process. Severe plastic deformation and high temperature in this area have led to complete recrystallization and severe microstructural changes in this area. As can be seen in Figure 14, in SZ both microstructural modification and fine-graining have occurred. To compare the difference in grain size in the weld nuggets of different specimens, the microstructure images of the weld nuggets of the welded specimens have been shown in Figure 15.

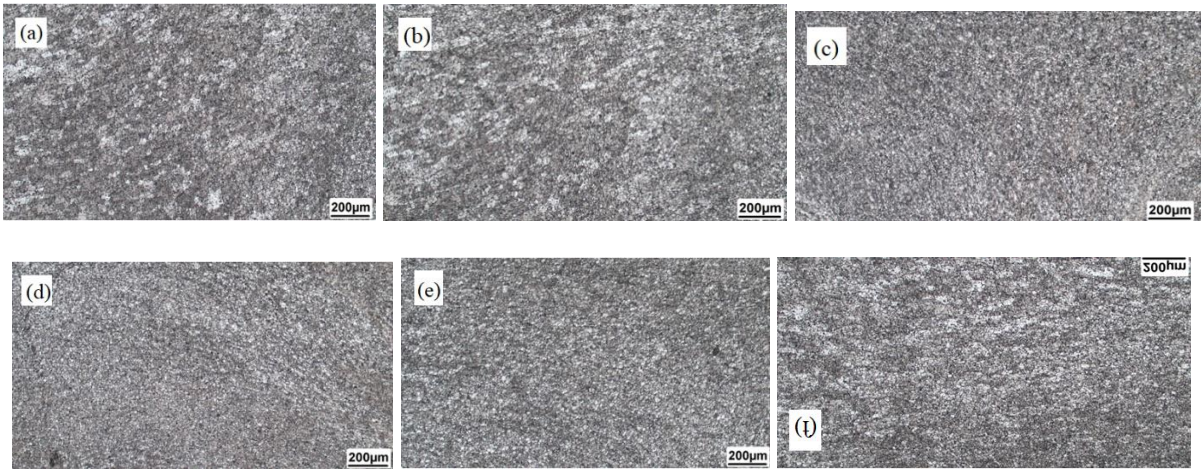

Figure 15. Grain size distribution for a) CF b) RP-D0 c) RP-D5 d) RP-D10 e) RP-D15 f) RP-D20

As can be seen in the RP-D10 and RP-D15 samples, recrystallization has occurred completely and growth of the grains has been formed uniformly and continuously throughout the section, which leads to the integration of the microstructural pattern of these samples in the weld nugget. These microstructural modifications and uniform distribution follow the results obtained from the tensile strength, flexural strength, and microhardness of these samples, which were presented in the previous

sections. According to Figure 15, it can be seen that in other welding specimens, recrystallization has occurred but the grain growth has not been uniform and the difference in grain size in the weld nugget of these specimens is visible.

5. Conclusion

The present study investigated the effect of using tools with tapered pins in Friction Stir Welding (FSW) of AA6061-T6 aluminum alloy. Two techniques named common FSW and RP- FSW backward were used for this purpose. Five tools with different tapered angles (0, 5, 10, 15 and 20 degrees) were used. To study the mechanical properties, tensile, three-point bending, and Vickers microhardness tests were performed. Macrographic and microstructural tests were also used to investigate the metallurgical properties of welded samples. Based on the results, it was found that:

1. The surfaces of all welded specimens with two different techniques (FSW and RP-FSW) were smooth and free of defects and there was no defect or lack of filling on the surface of any of the specimens.
2. In the welded specimens RP-D10 and RP-D15, the welded surfaces were smooth and perfectly integrated, and no visible protrusions or cavities were created in these specimens. However in the other four welded specimens, protrusions and flash defects have formed on the edges of the weld line.
3. The cross-section of all welding specimens except the CF specimen did not have common defects such as cavities and wormholes. In the CF sample, due to the asymmetry of the weld margin areas, the middle welding area at AS had a Wormhole defect.
4. According to the obtained results, it was found that changing the tapered angle of the tool significantly leads to changing the area of the SZ at the bottom of the welding area. It was observed that with increasing the tapered angle of the pin, the width of the SZ at the bottom of the workpiece decreased and also the total area of the SZ decreased.
5. Based on the results of the tensile test, it was found that the determining factor of ductility and strength of the welded specimens is the type of welding process (FSW or RP-FSW) and the pin geometry (simple or tapered pin).
6. It was found that all specimens welded by the RP-FSW method have higher UTS and elongation than the specimens welded by conventional FSW.
7. By increasing the tapered angle of the tool pin, the two mechanical properties of UTS and elongation of welded specimens by RP-FSW first increased with a significant slope and then decreased. In welded specimens, by increasing the tapered angle of the tool pin to an angle of 15 degrees, the UTS of welding specimens increased, but by increasing the angle by 15 degrees, it was observed that the UTS and ductility of the specimen decreased.
8. The decrease in welding efficiency at a tapered angle of 20 degrees is due to the reduction of plastic flow at the bottom of the workpiece. By increasing the tapered angle, the volume of horizontal flow formed in the lower surfaces of the workpiece gradually decreases due to decreasing pin diameter in these areas. This reduction in flow volume reduces the quality of the joint.
9. Based on the results, by using the tapered angle of 15 degrees of the tool pin, the optimal state of mechanical properties of the joint is provided. In this situation, two parameters of UTS and elongation, have experienced growth of 18.7% and 21.4% compared to the common state of P-FSW

(simple cylindrical pin of RP-D0), respectively. Also, 31.1% and 27.8% growth compared to the sample welded by FSW (CF), was observed, respectively.

10. Following the presented results, it was found that the choice of welding process type and type of tool used for welding significantly affects the flexural behavior of welded specimens in the three-point bending test.

11. Based on the results of three-point bending tests, it was found that all samples welded by the P-FSW method show better flexural behavior and have higher flexural strength compared to the sample welded by the conventional FSW method.

12. Based on the obtained results, out of six welded samples, two samples RP-D15 and RP-D10 did not fail to bend to the maximum deflection and showed a behavior similar to base metal.

13. It was observed that by increasing the tapered angle of the tool pin to an angle of 15 degrees, the amount of flexural strength and flexural length increment increases, but with increasing this angle from 15 degrees, the values of flexural strength and ductility of the sample decrease.

14. According to the results, among the welded specimens, the highest flexural strength belonged to the RP-D15 specimen. The flexural strength of this sample is 92.7% of the base metal. Also, by deliberating the results, it was found that the flexural strength of the RP-D15 sample has increased by 27.1% compared to the CF sample, and 16.4% growth compared to the RP-D0 sample was observed.

15. Based on the results of tensile and three-point bending tests it was found that among the tools used for P-FSW, tools with tapered angles of 15, 10, 5, 0, and 20 degrees, respectively, create the highest UTS and flexural strength.

16. Similar to FSW mode, in the conditions of using P-FSW, the hardness pattern in all welding specimens was almost W-shaped. In all samples, the hardness of SZ, TMAZ, and HAZ were significantly lower than the hardness of the base metal.

17. In all samples, the hardness of SZ was higher than the adjacent areas due to the presence of complete dynamic recrystallization in the SZ area, which leads to microstructure modification in this area.

18. Regardless of the type of tool used for welding, the lowest hardness values occurred at the HAZ in all samples.

19. Following the microhardness patterns observed in the specimens welded by the RP-FSW method, the hardness value of the SZ is directly dependent on the degree of tapered angle of the tool used. It was observed that tools with tapered angles of 15, 10, and 5 have the highest hardness values in the weld nugget, respectively.

20. It was observed that the lowest grain sizes in SZ, TMAZ, and HAZ belong to RP-D15, RP-D10, and RP-D5 welding specimens, respectively. Also, it was found that the trend in the average grain size in the two welding methods is close to the results obtained from the mechanical tests of tensile, three-point bending, and microhardness.

21. In specimens welded by the P-FSW method, due to the overlap created in the first and second passes, microstructural modification have increased, which has led to fine-graining in SZ.

6. References

[1] Hassanifard, S., Nabavi-Kivi, A., Ghiasvand, A. and Varvani-Farahani, A. 2021. Monotonic and fatigue response of heat-treated friction stir welded Al 6061-T6 joints: Testing and characterization. Materials Performance and Characterization. 10(1):353-369. doi.org/10.1520/MPC20200076.

[2] Li, J.Q. and Liu, H.J. 2013. Characteristics of the reverse dual-rotation friction stir welding conducted on 2219-T6 aluminum alloy. Materials & Design. 45:148-154. doi.org/10.1016/j.matdes.2012.08.068.

[3] Li, J.Q. and Liu, H.J. 2015. Effects of the reversely rotating assisted shoulder on microstructures during the reverse dual-rotation friction stir welding. Journal of Materials Science & Technology. 31(4):375-383. doi.org/10.1016/j.jmst.2014.07.020.

[4] Liu, H.J., Li, J.Q. and Duan, W.J. 2013. Research on reverse dual rotation friction stir welding process. In Proceedings of the 1st international joint symposium on joining and welding. Woodhead Publishing. doi.org/10.1533/978-1-78242-164-1.25.

[5] Shi, L., Wu, C.S. and Liu, H.J. 2015. The effect of the welding parameters and tool size on the thermal process and tool torque in reverse dual-rotation friction stir welding. International Journal of Machine Tools and Manufacture. 91:1-11. doi.org/10.1016/j.ijmachtools.2015.01.004.

[6] Thomas, W.M., Staines, D.J., Watts, E.R. and Norris, I.M. 2005. The simultaneous use of two or more friction stir welding tools. Abington, Cambridge, TWI.

[7] Liu, H.J. and Zhang, H.J. 2009. Repair welding process of friction stir welding groove defect. Transactions of Nonferrous Metals Society of China. 19(3):563-567. doi.org/10.1016/S1003-6326(08)60313-1.

[8] Kumari, K., Pal, S.K. and Singh, S.B. 2015. Friction stir welding by using counter-rotating twin tool. Journal of Materials Processing Technology, 215:132-141. doi.org/10.1016/j.jmatprotec.2014.07.031.

[9] Jain, R., Kumari, K., Pal, S.K. and Singh, S.B. 2018. Counter rotating twin-tool system in friction stir welding process: A simulation study. Journal of Materials Processing Technology. 255:121-128. doi.org/10.1016/j.jmatprotec.2017.11.043.

[10] Ghiasvand, A., Hassanifard, S., Jalilian, M.M. and Kheradmandan, H. 2021. Investigation of tool offset on mechanical properties of dissimilar AA6061-T6 and AA7075-T6 joint in parallel FSW process. Welding in the World. 65:441-450. doi.org/10.1007/s40194-020-01037-4.

[11] Gadakh, V.S. and Kumar, A. 2014. Friction stir welding window for AA6061-T6 aluminium alloy. Proceedings of the Institution of Mechanical Engineers, Part B: Journal of Engineering Manufacture. 228(9):1172-1181. doi.org/10.1177/0954405413510289.

[12] Hassanifard, S., Alipour, H., Ghiasvand, A. and Varvani-Farahani, A. 2021. Fatigue response of friction stir welded joints of Al 6061 in the absence and presence of inserted copper foils in the butt weld. Journal of Manufacturing Processes. 64:1-9. doi.org/10.1016/j.jmapro.2021.01.010.

[13] Callister Jr, W.D. and Rethwisch, D.G. 2020. Callister's Materials Science and Engineering. John Wiley & Sons.